Characterization of Contemporary and Historical Acrylonitrile Butadiene Styrene (ABS)-Based Objects: Pilot Study for Handheld Raman Analysis in Collections

Daniela Reggio,[a,b] Daniela Saviello,[c] Massimo Lazzari[a,b] and Daniela Iacopino[c*]

[a]Departamento de Química Física, Facultade de Química, Universidade de Santiago de Compostela, Santiago de Compostela, Spain

[b]Centro Singular de Investigación en Química Biolóxica e Materiais Moleculares, (CiQUS)

[c]Tyndall National Institute, University College Cork, Nanotechnology group, Dyke Parade, T12R5CP, Cork (Ireland)

*corresponding author email: daniela.iacopino@tyndall.ie

Abstract

Plastic materials are increasingly becoming part of private and public collections worldwide, either as design objects or artistic sculptures. The preservation of these highly degradable materials requires novel analytical approaches able to reveal their chemical composition to inform the tailoring of appropriate conservation procedures. In this work Raman spectroscopy and Surface-enhanced Raman Scattering (SERS) were proposed as methods for the characterization of ABS-based contemporary and historical LEGO® objects. Twenty-three objects of twelve different colors were analyzed by handheld and benchtop Raman instrumentation. In all cases clear identification of the constituent polymer matrices (ABS, polycarbonate, poly(methyl metacrylate)) was obtained. In addition, identification of major color components was achieved, such as copper phthalocyanines in green and blue objects. Low cost handheld instrumentation provided acceptable sensitivity towards polymers and coloring media, and was found suitable for initial screening of the objects. Benchtop Raman was used to confirm and further extend identification, as well as for building background information. Finally, SERS sensitivity was found comparable to the sensitivity achieved by benchtop Raman instrumentation. However, the associated minimally-invasive sampling method made SERS a valid alternative to direct Raman spectroscopy for the analysis of immovable and/or large-sized objects. Overall, this work represents the first systematic investigation on the potential of Raman and SERS spectroscopies as methods for minimal invasive and/or *in situ* analysis of historical and contemporary plastic objects.

Keywords: ABS; LEGO; synthetic organic pigments (SOPs); Surface-enhanced Raman Scattering (SERS), Raman spectroscopy; handheld Raman; contemporary art.

1. Introduction

Since the end of the 19th century the versatility, good workability, easiness of coloration, and low cost of plastic materials has been exploited by artists, designers and architects to create artworks and objects today part of many museum collections [1,2]. Unfortunately, the chemical instability of plastic towards air, moisture, light and heat causes degradation, resulting in deformation, shrinkage, cracking, changes in color and gloss in few decades [3-5]. The development of appropriate preservation strategies should start from the identification of the object constituent materials. However, rarely heritage objects in collections have a complete set of information on chemical composition and fabrication methods. Therefore, there is an increasing need of developing analytical methods enabling fast and reliable analysis of polymeric materials [6]. Ideally such methods would include tools to detect early degradation markers and allow clear identification of plastic components such as pigments, dyes, additives, stabilizers and fillers [7, 8]. In fact, these components possess their own chemical stability and degradation patterns, which can alter the overall weathering mechanism of the object [9-11].

Acrylonitrile butadiene styrene (ABS) is a copolymer made of an acrylonitrile–styrene continuous phase (SAN) and partially grafted polybutadiene (PB) that acts as an impact modifier, giving excellent mechanical properties to the material [12]. ABS is the constituent polymer of many design and collection objects [2, 13, 14], as well as contemporary artworks [15]. Furthermore, as ABS is a widely used rapid prototyping material within the artistic community [16], it is expected that a large number of 3D printed ABS artworks will be found in museums in the next decades. Among ABS objects, LEGO® toys are increasingly becoming cult objects, being part of numerous private and museum collections. The first LEGO® factory was funded by Christiansen in Denmark in 1932 [17, 18, 19]. Initially producing wooden block toys, the factory switched to cellulose acetate (CA) in 1953, following Hilary Page's patent on self-locking building blocks toys made with injection molding machines filed in the United Kingdom back in 1939 [20]. However, the turning point of LEGO® success was linked to Christiansen's patent (US/Denmark, 1958) introducing tubular self-clinching studs to connect objects [50, 51]. The switch from CA to ABS started in 1962, motivated relatively low cost, easiness to mold accurately, colorfastness and mechanical stability of ABS [21, 22]. Since then, the initial color palette has considerably widened from the original seven colors (white, grey, black, red, blue, yellow and green) to the fifty-seven colors used in contemporary formulations [23]. Unsupported data suggest that MACROLEX® thermoplastic colorants are currently the constituents of twenty-five colors currently being produced by LEGO® [24]. Elsewhere, Laxess Chemicals dyes and INEO Styrolution ABS pellets [25, 26] are mentioned. However, to date no systematic scientific literature is available on the chemical composition of contemporary and historical LEGO® objects.

Characterization of polymeric components in plastic objects is traditionally performed with a number of analytical techniques, such as pyrolysis-gas chromatography mass spectrometry (Py-GC/MS) [27-29], nuclear magnetic resonance (NMR) [30, 31], vibrational spectroscopies as infrared in mid and

near infrared region (MIR and NIR) [32-34] and Raman [35-37]. In the last decades, Raman and Surface-enhanced Raman Scattering (SERS) have been extensively used in museum contexts to identify pigments and dyes in paintings and paper media, but the application of such techniques for identification of colorants in polymer matrices is largely underexplored [38-42]. Analytical evidence from benchtop instrumentation is often considered more reliable than evidence acquired with portable instrumentation to address object condition state, conservation treatments, ongoing weathering mechanisms, and optimal preservation strategies [43]. However, benchtop instrumentation is not suitable for *in situ* analysis of large-sized objects. Therefore, as conservation scientists face the challenge to answer research questions on materials, while facing ethical limitations on invasive sampling, the use of Raman handheld instrumentation with *in situ* measurement capabilities could constitute a good compromise to preserve the integrity of objects under examination [44, 45]. However, a systematic comparative study of the merits and limitations of Raman handheld and benchtop instrumentations for analysis of plastic materials is to date largely missing.

This paper constitutes the first example of systematic application of Raman and SERS spectroscopies for the identification of plastic, constituent synthetic organic pigments (SOPs) and complex inorganic colored pigments (CICPs) in contemporary and historical ABS objects. The aim of this pilot study was to optimize a method for minimal-invasive sampling combined with non-invasive analysis of plastic art and design objects in collections. LEGO® toys were selected as a model ABS material, due to the easy access to contemporary and historical colored objects at low costs [23]. Moreover, given their iconic cultural impact, LEGO® objects have been used by contemporary artists such as Nathan Sawaya and Ai Wewei as an art medium [46-49]. Contemporary LEGO® objects were comparatively examined with three instrumental settings: non-invasive handheld Raman spectrometer for initial screening, non-invasive benchtop Raman spectrometer to obtain finer spectral features, and finally minimally invasive SERS as method alternative to Raman handheld. Historical LEGO® objects were analyzed only by non-destructive and non-invasive handheld and benchtop Raman instrumentation in order to preserve their integrity, as it should be preferred by analysts in museum contexts [44]. Complementary ATR-FTIR was also performed to support obtained results in this exploratory phase. The knowledge gained through this systematic study, both in terms of chemical composition and assessment of technique/instrumentation capability, is highly relevant to support future wider applications of minimally-invasive Raman and SERS techniques for the analysis of other ABS contemporary and historical objects in museum and collection settings. The analysis of contemporary and historical ABS objects revealed the ability of handheld Raman instrumentation to discriminate major polymer and colorant components *in situ* and in a non-invasive manner for both contemporary and historical objects. This capability is of key importance in museum settings to perform fast screening of objects towards assessment of their chemical composition.

2. Materials and Methods

2.1 Materials

Contemporary LEGO® objects dated 2015 (The Lego Group, Billund, Denmark), were purchased from a local store in Ireland. Historical objects were borrowed from a private collection purchased in Ireland between 1972 and 1979. The sixteen contemporary LEGO® objects analyzed and the seven historical objects analyzed are listed in Table 1. A commercial ABS film 100 µm thick obtained by extrusion from Magnum 3404 pellets was purchased from Dow Chemicals (Dow Chemical Company Midland, MI, USA) and used as a reference material.

2.1.2 SERS substrates fabrication

SERS substrates were produced by a procedure described in detail elsewhere [50, 51]. Briefly, ultraviolet nanoimprint soft lithography (UV-NIL) through a roll-to-roll procedure was used to fabricate nanometric periodic structures then coated with 150 nm of Al by physical thermal vapor deposition (PVD). Fluorolink MD700 was the UV curable fluorinated pre-polymer used in combination with 2-methoxy-2-phenylacetophenone photo-initiator. The master replica mold was an elastomeric silicone hollow (SYLGARD 184 by Dow Corning, INC, US) supporting a nanostructure with pillars in hexagonal array with an approximate size of 220 nm diameter and 450 nm pitch (FleFimo™ tape by Soken Mold Solution).

2.2 Spectral analysis

2.2.1 Colorimetric analysis

Color measurements were performed with a portable Konica Minolta CM 700d spectrophotometer (Konica Minolta, INC., Tokyo, Japan). Color space was the CIE L*a*b* with D65 standard illuminant and 10° observer, SAV 3/6 ø mm illumination area. SpectraMagic NX software was used for a comprehensive color analysis. The coordinates reported in Table 1 refer to the diffuse reflectance spectra (specular component excluded - SCE), correlating the aspect of the color observed to the coordinates without gloss effects.

2.2.2 Raman spectroscopy

Handheld Raman spectra were obtained from a DeltaNu PharmaID spectrometer (Pharma-ID Ltd, UK) with illumination at 785 nm, spectral range 300 -2400 cm^{-1} and spectral resolution 10-12 cm^{-1}. The laser power was 50 mW and typical acquisition time was between 0.2 and 10 s. An average of five measurements was taken in different parts of the sample. Representative spectra were reported in the main manuscript.

A Renishaw (Renishaw PLC, UK) benchtop InVia Flex with spectral range 100 -3200 cm^{-1} and spectral resolution 0.5 cm^{-1}, 1200 mm^{-1} grating lines, CCD 576 x 400 pix detector, and equipped with a 785 nm laser was used to collect benchtop Raman and SERS spectra. Accumulation time was 10 sec and laser powers spanned from 1 to 5% corresponding to 9-45 mW powers. A long working distance Leica objective (model 5660036) operated with a 65 µm slit opening. The same instrumentation was used

to perform SERS measurements. Fragments of sub-micron size (ca 0,1 - 1 mg) were sampled with a scalpel from the inner surface of LEGO® objects, then solubilized in glass vials with 2 mL of ≥ 99,8 % anhydrous chloroform stabilized with 100 ppm of amylene to extract color components and polymer [50, 51]. Lambda Plus Single Channel Pipettor (0,2-2 µL volumes) was employed to accumulate on the SERS substrate approximately two drops, each of 0,75 µL, followed by complete solvent evaporation for spectral acquisition. An average of five measurements was collected on the concentrated drop deposited on the SERS substrate. Representative spectra were reported in the main manuscript.

Spectral libraries IRUG and Soprano were used as support for the identification of colorant components in recorded experimental Raman and SERS spectra [52, 53].

2.2.3 FTIR spectroscopy

ATR-FTIR tests were carried out with a benchtop Thermo Nicolet 6700 (Thermo Fisher Scientific, US) with Smart Endurance device with an Hg-Cd telluride (MCT) detector at 4 cm^{-1} resolution for 128 scans. Samples (1 – 4 mg) were removed from the inner part of the objects examined with a scalpel. Ominic 7 and Origin 9.1 software were used to process and plot Raman and FTIR data.

3. Results and Discussion

Table 1 shows the list of twenty-three analyzed LEGO® objects, including sixteen contemporary and seven historical objects. For all objects an identification name, description, size and L*a*b coordinates are presented. The numbers in bracket in the “Type” column represent the numerical classification based on number of studs (short side X long side). Figure 1 shows a photographic image of all analyzed objects.

Table 1. List of analyzed LEGO® objects including name, dating, size and color coordinates.

Object Name	Dating	Type	Length X width X thickness (mm)	Color coordinates (CIE)		
				L*	a*	b*
Black1	2015	Brick (1 X 1)	15.5 X 7.5 X 11	13.28	-0.45	-2.37
White3	2015	Brick (1 X 1)	15.5 X 7.5 X 11	83.10	0.24	5.65
Pink1	2015	Brick (2 X 4)	32 X 16 X 12	75.57	26.31	-12.45
Grey2	2015	Brick (2 X 3)	23 X 15 X 10	57.48	1.18	1.25
Brown1	2015	Brick (2 X 3)	23 X 15 X 10	45.46	9.61	8.23
Wine1	2015	Brick (2 X 2)	17.5 X 17.5 X 12	44.96	18.92	9.55
Blue1	2015	Plate (2 X 6)	33 X 16 X 5.5	39.89	-9.52	-41.32
Blue5	2015	Wedge (2 X 2)	17.5 X 17.5 X 12	67.94	-34.17	-19.87
Green1	2015	Brick (2 X 2)	17.5 X 17.5 X 12	42.73	-62.30	30.12
Green3	2015	Wedge(1 X 1)	15.5 X 7.5 X 11	69.18	-19.23	69.48
Colorless1	2015	Wedge (1 X 1)	15.5 X 7.5 X 11	-	-	-
Black4	2015	Plate with wheels (2 X 2)	17.5 X 18 X 12	13.31	-0.20	-0.76
Yellow	2015	Cylinder (2 X 2)	16,5 X 12	79,87	7,44	84,12
Red	2015	Brick (2 X 4)	23 X 15 X 10	51,69	26,62	14,81
Purple	2015	Brick (1 X 1)	15.5 X 7.5 X 11	31,11	25,48	-41,36
Grey5	2015	Brick with propeller (2 X 4)	23 X 15 X 5.5	57,48	-1,18	-1,25
Green7	1972- 1979	Brick (2 X 6)	69 X 34 X 22	51.57	-42.22	18.54
Blue6	1972- 1979	Brick (2 X 4)	33.5 X 16 X 12	49.62	-20.14	-17.11
Grey3	1972- 1979	Plate (2 X 8)	65 X 16 X 5.5	64.16	-2.13	2.68
White1	1972- 1979	Brick (2 X 4)	33.5 X 16 X 12	87.48	2.45	18.65
Colorless 2	1972- 1979	Brick (2 X 2)	16.5 X 16.5 X 12	-	-	-
Yellow	1972- 1979	Brick (2 X 2)	17.5 X 17.5 X 12	79,04	10,07	69,17
Red	1972- 1979	Brick (1 X 1)	15.5 X 7.5 X 11	44,71	47,19	27,82

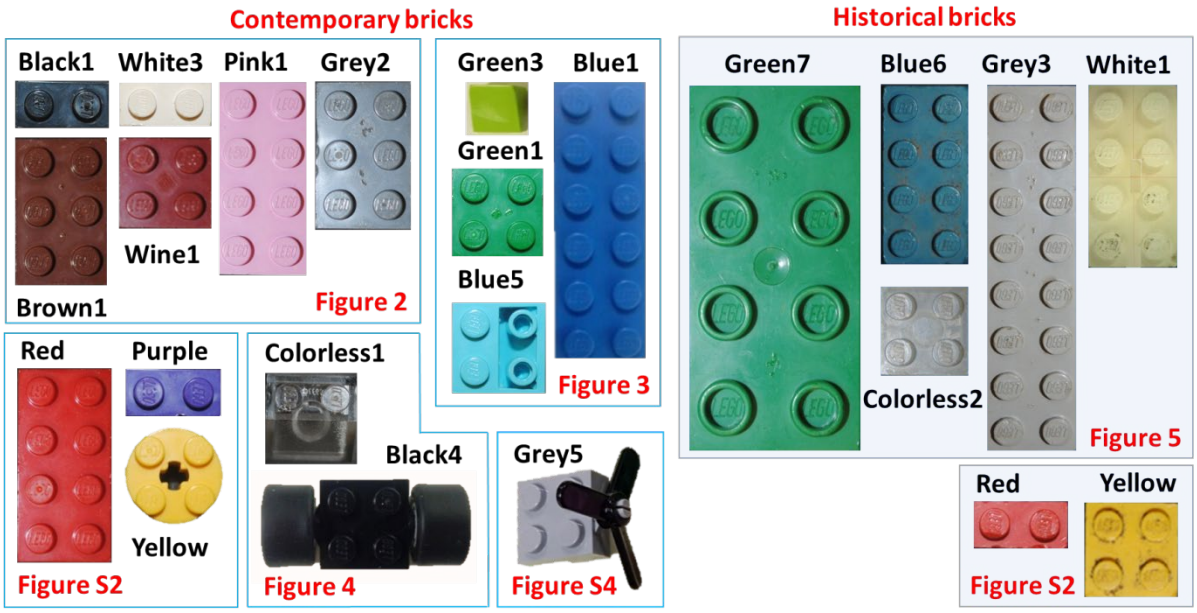

Figure 1. Photograph of analyzed contemporary and historical LEGO® objects.

Prior to analyses of ABS colored objects, Raman (handheld and benchtop instrumentations, Figure 1a,b) and SERS (benchtop instrumentation, Figure 1c) spectra of a commercial film were acquired as reference spectra for subsequent measurements. All ABS Raman spectra were characterized by a main band at 1003 cm^{-1}, attributable to the benzene ring breathing vibration from the styrene acrylonitrile (SAN) part of ABS. Additional bands attributable to vibrations of the aromatic ring were found at 1005 and 1035 cm^{-1}. The complete list of bands and assignments of the spectrum recorded with Raman benchtop instrumentation is shown in Table S1 and Figure S1.

As the use of Raman handheld instrumentation allows a rapid non-invasive screening of objects, a low cost and light-weight handheld spectrometer was firstly employed to take Raman spectra of colored ABS brick and to assess its diagnostic capabilities. Figure 2a shows Raman spectra recorded with handheld instrumentation. The majority of spectra displayed good resolution. ABS bands centered at 1005 and 1035 cm^{-1} were visible in all objects, except for Black1 which showed a noisy spectrum with unidentifiable features. In addition, other bands attributable to either CICPs or SOPs used to achieve the desired coloration were observed in most spectra. Such features were marked with an asterisk in the spectra to distinguish them from the ABS bands. Specifically, bands attributable to the presence of TiO_2 were visible in White3, Pink1 and Grey2 spectra at ca. 412 and 620 cm^{-1}, overlapping with ABS bands but showing more intense features. Brown1 and Wine1 displayed non-ABS features at 409 and 505 cm^{-1}, attributable to Pigment Brown 29 (PBr29 - C.I. 77500), an inorganic pigment of black mixed iron (III) oxide and chrome (III) ($(Cr,Fe)_2O_3$) within an hematite structure [54].

In order to better assess merits and limitations of handheld instrumentation, an equivalent analysis was performed with benchtop instrumentation and recorded spectra are shown in Figure 2b. All analyzed objects displayed strong bands at 620, 1003, 1032, 1185, 1200, 1451 and 1603 cm^{-1} attributable to ABS. For these spectra also additional bands associated either to CICPs or SOPs were observed for all objects. As in Figure 2a, such additional bands were marked with black asterisks to distinguish them from the ABS bands. Specifically, Black1 and Grey2 objects showed bands attributable to the presence of carbon black (CB) with a typical vibration centered at 1302 cm^{-1} and a broadened band at 1599 cm^{-1} overlapping with the symmetric stretching vibration of the benzene ring from ABS. White3, Pink1 and Grey2 objects showed a shoulder at 610 cm^{-1} and an additional band at 445 cm^{-1} associated to the presence of TiO_2. For Pink1 the broad band at 445 cm^{-1} showed a higher relative intensity compared to the other spectra where TiO_2 was also detected. Bands centered at 222, 292 and 411 cm^{-1} in Brown1 and Wine1 were identified as the dark brown and the reddish shades of Pigment Brown 29 (PBr29 - C.I. 77500), an inorganic pigment of black mixed iron (III) oxide and chrome (III) ($(Cr,Fe)_2O_3$), within an hematite structure [54, 55]. Direct comparison of spectra taken by handheld and benchtop instrumentation showed that in spite of the lower spectral resolution and smaller spectral window, handheld instrumentation performed satisfactory characterization of ABS materials.

As an alternative method, also SERS measurements were performed to test its suitability for the identification of coloring media in complex polymeric matrices, namely plastics used for contemporary artworks and design objects. As shown in Figure 2c, clear spectral signals were obtained for all objects analyzed. The position and intensity of bands obtained was ca. equivalent to those obtained by Raman benchtop analysis, thus further confirming previous assignments. Bands associated to the presence of TiO_2 at 443 cm^{-1} and C black at 1301 and 1603 cm^{-1} in Grey2 presented enhanced features compared to features obtained by Raman benchtop. These data confirm the capability of SERS to generate high intensity spectral features from sub-micrometric sampling through a simple one-step procedure. Hence the method is suitable for museum collections analysis, whereby instrumentation for *in situ* analysis might not always be available and sampling must be kept minimal to preserve the integrity of the analyzed object. The ability to obtain high quality spectra from minimal-invasive sampling is an important aspect. In fact, although the high sensitivity of SERS for the characterization of colorant and colorant mixtures in objects has been widely reported, its practical application is still limited by the need for extraction procedures, usually performed by complex three/four steps procedures with hazardous chemicals [39, 41].

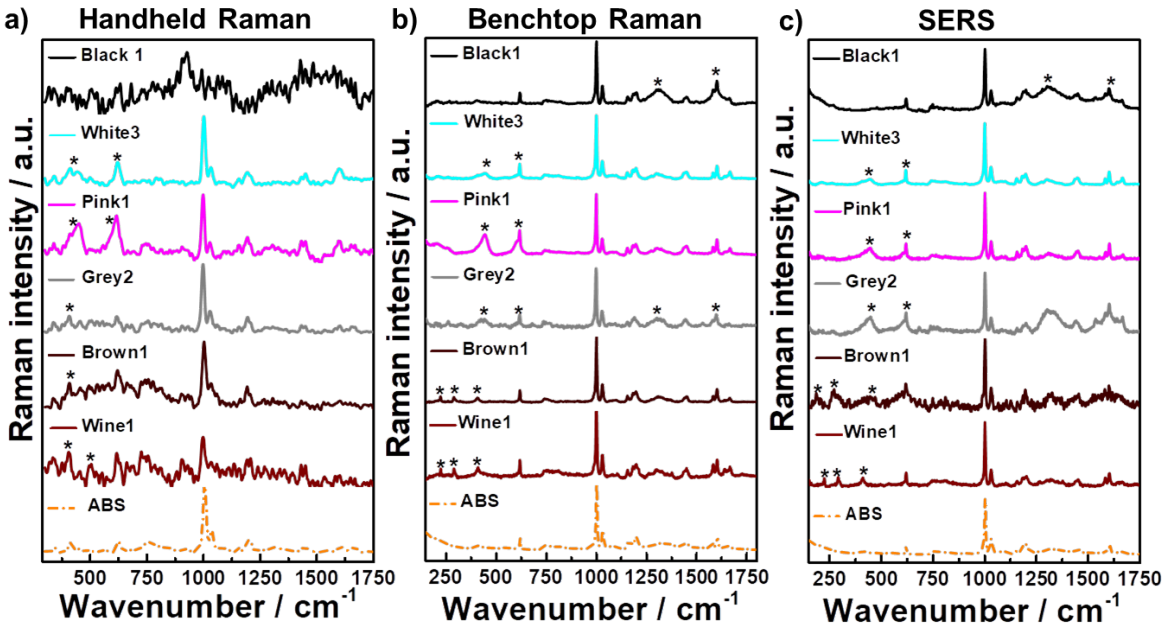

Figure 2: Spectral analysis of contemporary colored ABS objects and reference ABS. a) Handheld Raman spectra; b) Benchtop Raman spectra; c) SERS spectra recorded with benchtop Raman instrumentation. All spectra were recorded with 785 nm wavelength illumination. Black asterisks indicate colorant component bands.

Interestingly, Raman and SERS spectroscopies also proved effective in chemical differentiation of pigments used to achieve similar color hues such as those used in dark and light blue- and green-colored objects. Figure 3a shows handheld Raman spectra of such objects. The spectrum of Blue1 showed strong bands associated to the presence of Copper Phthalocyanine (CuPc) pigments centered at 489, 680, 746, 1141, 1337, 1524 cm^{-1}, likely Pigment Blue 15 (PB15, C.I. 74160). Such pigment belongs to the family of green and blue copper phthalocyanine SOPs, commonly used in paint formulations due to their high performance in stability, resistance to migration and good transparency [56, 57]. The Raman spectrum of Blue5 showed bands at 685, 745, 1144, 1195, 1340 and 1529 cm^{-1}, also associated to the presence of CuPc SOPs, likely PB15. The spectrum of Green1 showed bands attributed to Pigment Green 7 (PG7, C.I. 74260), a chlorinated CuPc commonly used in plastics for its excellent light fastness and dispersion properties at 682, 739, 779, 818, 1082, 1212, 1340 and 1538 cm^{-1}. Green3 also showed bands characteristics of the presence of PG7 at 1533, and 742 cm^{-1} [52, 53]. Analogously to the analytical procedure showed in Figure 2, benchtop Raman and SERS analyses were performed on these objects to assess limitations of handheld instrumentation. The Raman benchtop spectrum of Blue1 (Figure 3b) showed spectral features attributable to ABS at 1003 and 1032 cm^{-1}. In contrast to spectra of other colored objects shown in Figure 2b, whereby ABS bands constituted the predominant features, ABS bands in Blue1 showed relatively small intensity. In fact, the Raman spectrum of Blue1 was dominated by strong additional bands centered at 481,

677, 744, 777, 950, 1104, 1142, 1340 and 1529 cm^{-1}, confirming the presence of a blue copper phthalocyanine dye (CuPc), likely Pigment Blue 15 (PB15, C.I. 74160) [52, 53; 56,57]. The Raman spectrum of Blue5 showed strong similarities with the spectrum of Blue1. Specifically, in addition to more pronounced ABS features, the following bands were observed, centered at 680, 747, 1142, 1340 and 1529 cm^{-1}, also suggesting the presence of CuPc dyes. Initially the polymorph β-CuPc (PB15:3) was identified in Blue5 from comparison with spectral databases and diagnostic spectral shifts [56, 57]. However, CuPc polymorphs present similar spectral features and in complex matrices where contributions from other components are present, spectral shifts are not sufficient to support a reliable discrimination. Band intensities also vary between CuPc polymorphs and therefore intensity ratios are used as more reliable polymorphic markers [57]. Specifically, the presence of PB:15(0) and PB:15:3 in Blue1 and Blue5 might be confirmed by the calculation of intensity ratio of bands at 749 and 679 cm^{-1} which was equal to 1.5 and 1.1 for Blue1 and Blue 5, respectively. These values are in agreement with values reported by Defeyt *et al.* for Raman identification studies of CuPc used in modern artist paints [57]. For clarity, bands attributed to CuPc pigments were marked with black asterisks in the spectra. Similar analysis was also carried out for two shades of green, also shown in Figure 3b. The spectrum of Green1 showed bands at 264, 288, 346, 644, 686, 738, 778 818, 1081, 1212, 1276, 1340, 1537and cm^{-1} which were attributed to Pigment Green 7 (PG7, C.I. 74260) [52, 53]. On the other hand, the light green Green3 brick presented intense ABS features and also showed bands characteristics of CuPc compounds at 660, 747, 1378, and 1537 cm^{-1}, which were attributed to presence of Pigment Green 36 (PG36, C.I. 74265) [52, 53]. The identification of CuPc polymorphs was obtained also by direct comparison of corresponding reference spectra from Raman spectral libraries [52, 23]. Blue and green objects SERS spectra are shown in Figure 3c. SERS spectra of good intensity were obtained for all colors, clearly showing presence of CuPc pigments in the objects formulations. Compared to Raman spectra, the ratio between the intensity of ABS bands and the intensity of colorant bands increased, showing that the ABS component was more easily extracted in $CHCl_3$ than the CuPc component, due to the latter poor solubility in organic solvents. However, clear presence of the CuPc SOPs was still observed, as shown by the number of bands marked with black asterisks in the spectra. It should also be mentioned that additional Raman (handheld and benchtop) and SERS measurements were also carried out on red, purple and yellow colored objects (Figure S2). For all samples ABS spectral contribution was evident, but no conclusive identification of SOPs was obtained.

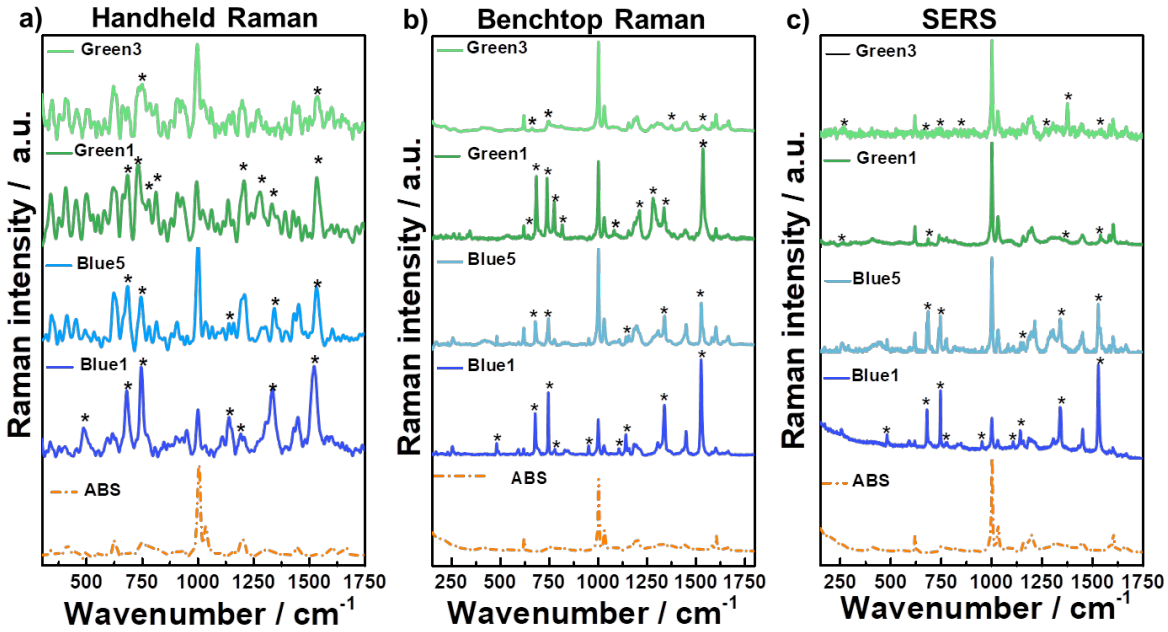

Figure 3: Spectral analysis of contemporary green and blue colored ABS objects and reference ABS. a) Handheld Raman spectra; b) Benchtop Raman spectra; c) SERS spectra recorded with benchtop Raman instrumentation. All spectra were recorded with 785 nm wavelength illumination. Black asterisks indicate colorant components bands.

Although it is known that ABS is the main polymer used in LEGO® objects formulations, the use of Raman instrumentation allowed the identification of some cases in which alternative polymers or polymer blends were used to enhance mechanical properties and color of the objects [23]. Figure 4 shows Raman and SERS spectra of Colorless1 and Black4 objects, in which different polymer formulations have been found. Specifically, in Colorless1 the strongest contribution was given by the presence of polycarbonate (PC) which characteristic bands were observed at 404, 636, 705, 734, 823, 887, 919, 1111, 1178, 1184, 1237, 1448, 1463, 1603 and 1778 cm^{-1} in both Raman and SERS spectra [58]. For clarity, PC bands were marked by red asterisks in the Colorless1 Raman spectrum. PC achieves superior transparency and presents lower yellowing with ageing [59]. In another example, the Raman and SERS spectra of Black4 also showed Raman bands attributable to PC at 404, 634, 708, 732, 832, 890, 922, 1008, 1109, 1179, 1237, 1448, 1465, 1603 and 1773 cm^{-1}. Black4 also showed broadened bands at 1603 and 1303 cm^{-1} attributable to CB (marked by black asterisks). In this case it has been hypothesized that the use of PC was intended to impart additional mechanical features to the brick (e.g. tensile and flexural strength, elasticity, hardness), as the piece was built to support the wheel attachment. This hypothesis was confirmed by the fact that the Raman spectrum of plain brick Black1 shown in Figure 2a did not show any additional polymer to ABS. ATR-FTIR data for Black1 and Black4 shown in Figure S3 confirmed the Raman attributions. The hypothesis related to enhanced mechanical properties was also supported by the analysis of another grey brick, Grey5, built to allow optional propeller attachment which Raman spectrum also showed presence of PC (Figure S4). As

already observed for the previously analyzed colored ABS objects, spectra obtained by Raman and SERS showed comparable band intensity and resolution.

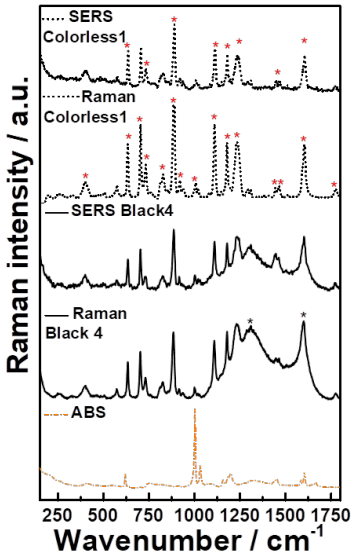

Figure 4: Raman and SERS spectra of Colorless1 and Black4 containing additional polymers to ABS. Both spectra were taken with benchtop instrumentation at excitation wavelength 750 nm.

Finally, historical 1970's LEGO® objects were also analyzed to test the reliability of Raman handheld and benchtop instrumentation for polymer and colorants identification on naturally weathered samples. Five historical objects were selected with colors corresponding to previously analyzed contemporary objects (see Figure S2 for spectra of red and yellow historical objects). From an initial visual inspection of the photographs shown in Figure 1, superficial scratches and dirt residues were observed in all historical objects. Direct comparison with contemporary objects suggested photo-oxidation induced color alterations, particularly evident in the yellowed White1 and Colorless2 objects.

Handheld Raman spectra of historical objects are shown in Figure 5a. Green7 showed CuPc PG7 bands already found in contemporary Green1 with diagnostic bands at 637, 820, 1212, 1397 and 1534 cm^{-1}. Also CuPc was identified in Blue6 from bands at 684, 1124, 1337, and 1528 cm^{-1}. Presence of TiO_2, already found in contemporary White3 and Grey5, was confirmed for White1 and Grey3 from the bands at 442 and 617 cm^{-1}. Colorless2 brick showed the following bands attributable to poly(methylmethacrylate) (PMMA), marked with red asterisks in Figure 5b: 484, 593, 707, 745, 815, 964, 992, 1186, 1274, 1303, 1448, and 1734 cm^{-1} [60].

Benchtop Raman spectra of historical objects are shown in Figure 5b. Historical Green7 and Blue6 showed presence of CuPc PG7 and PB15, as previously found in contemporary objects. Similarly, presence of TiO_2 previously detected in contemporary objects was confirmed for White1 and Grey3

from bands 440 and 615 cm^{-1}. Raman spectrum of the Colorless2 brick showed the following bands attributable to PMMA) marked with red asterisks in Figure 5b: 484, 593, 707, 745, 815, 842, 913, 964, 992, 1186, 1274, 1303, 1448, 1646 and 1734 cm^{-1} [60]. To the best of our knowledge, there is no published evidence that explains the technological choice to substitute the blend of ABS and PMMA (historical brick, Figure 5) with plain PC (contemporary brick, Figure 4) for the fabrication of transparent LEGO® objects during the last forty years. However, in both cases gloss and transparency were the main features to achieve. Conclusive evidence on the oxidation of Colorless2 could not be determined because of the overlap of PMMA bands with ABS diagnostic bands for potential identification of oxidation [59, 60]. As no evidence of degradation can be discussed, the macroscopic change in color/yellowing observed in the historical objects compared to the contemporary objects was ascribed to the well-known poor yellowing performance of ABS reported in several publications [7, 59, 61]. Further color identification in historical objects is provided by spectra collected with handheld Raman instrumentation and comparison with spectral databases (Figure S2).

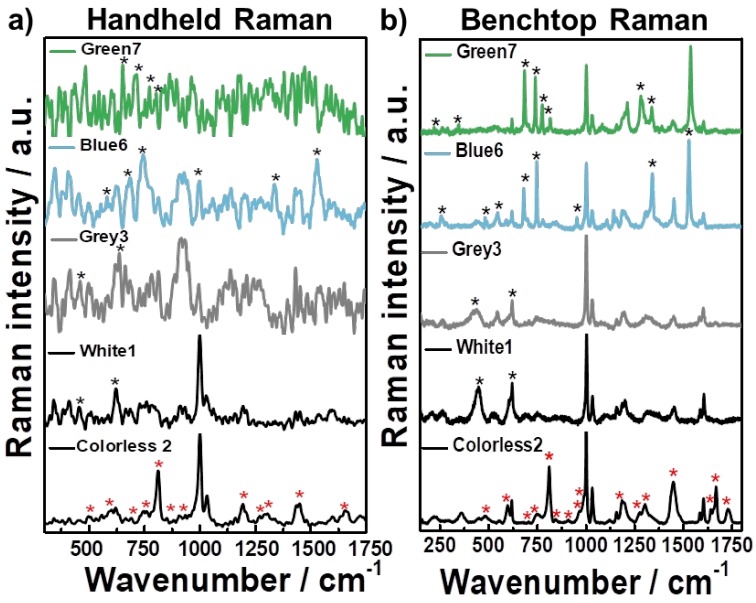

Figure 5. Spectral analysis of historical colored ABS objects and reference ABS. a) Handheld Raman spectra; b) Benchtop Raman spectra. All spectra were recorded with 785 nm wavelength illumination. Black asterisks indicate colorant components bands. Red asterisks denote PMMA bands.

A summary of polymer and colorants identified in analyzed contemporary and historical objects is reported in Table 2.

Table 2. List of analyzed contemporary and historical objects and identified polymer/colorant components.

Object Name	Identified polymer/ color component
Contemporary	
Black1	ABS, CB
White3	ABS, TiO_2
Pink1	ABS, TiO_2
Grey2	ABS, C black, TiO_2
Brown1	ABS, PBr29, $(Cr,Fe)_2O_3$
Wine1	ABS, PBr29, $(Cr,Fe)_2O_3$
Blue1	ABS, CuPc (PB15)
Blue5	ABS, CuPc (PB15:3)
Green1	ABS, CuPc (PG7)
Green3	ABS, CuPc (PG36)
Colorless1	ABS, PC
Historical	
Black4	PC, CB
Green7	ABS, CuPc
Blue6	ABS, CuPc
Grey3	ABS, TiO_2
White1	ABS, TiO_2
Colorless2	ABS, PMMA

4. Conclusions

This work represents the first example of systematic chemical characterization of contemporary and historical LEGO® toys performed by Raman spectroscopy, combining Raman handheld and benchtop instrumentation, as well as SERS optimized for minimal-invasive analysis. The aim of the work was to provide the foundations for the spectroscopic interpretation of complex colored polymeric matrices, assessing merits and limits of each technique and their potential for fast and reliable analysis of museum objects. Benchtop Raman instrumentation was effective for the non-invasive and non-destructive identification of the main polymer and pigments, proving enough sensitivity even to identify subtle chemical compositional differences between similar color hues (green and blue phthalocyanines). At a first glance SERS analysis showed sensitivity comparable to benchtop Raman analysis. However, the great advantage of SERS relied on the use of a novel minimal-invasive sub-micrometric sampling. This alternative approach is extremely desirable in museum settings and could well replace conventional Raman spectroscopy, when portable instrumentation is not available and/or does not provide reliable data. These results can be extended to historical plastic objects, not sampled in this pilot study to preserve the integrity of the material. Experimental results and methodological approach presented are recommended in real museum decision-making scenario: the initial screening of the object examined should be performed by non-invasive handheld

instrumentation; if the chemical identification of pigments and dyes dispersed in the polymeric matrix is inconclusive, then minimal-invasive SERS should be performed.

Conflicts of interest

There are no conflicts to declare.

Acknowledgements

This work was funded by the European Union H2020 project Nanorestart (646063),the Irish Research Council (IRC) project GOIPD/2015/716, the Xunta de Galicia (Centro singular de investigación de Galicia accreditation 2016–2019, ED431G/09; Consolidación e estructuración ED431B 2018/16) and the European Union (European Regional Development Fund—ERDF)

References

1. M. T. Baker, Polymers in Museums. In Historic Textiles, Papers, and Polymers in Museums, Cardamone, J. M., and Baker, M. T. (Eds). ACS Symposium Series 779. American Chemical Society: Washington, DC, 2000, pp. 128–135. ISBN 9780841218451 (ebook).
2. S. Katz, Plastics: Common Objects, Classic Designs; with a Collector's Guide. H.N. Abrams: New York, United States, 1984. ISBN 0-8109-0769-0.
3. B. Lavédrine, A. Fournier, G. Martin, Preservation of Plastic Artefacts in Museum Collections, CTHS EDITION, Comité des travaux historiques et scientifiques - CTHS, Paris, 2012. ISBN-10: 273550770X.
4. Y. Shashoua, Conservation of plastics: materials science, degradation and preservation. Elsevier/Butterworth-Heinemann, 2008. ISBN-10: 0750664959.
5. B. Singh N. Sharma, Mechanistic implications of plastic degradation. Polymer degradation and stability, Polym. Degrad. Stabil. 9 (2008), 561-584. DOI: 10.1016/j.polymdegradstab.2007.11.008.
6. D. Saviello, L. Toniolo, S. Goidanich, F. Casadio, Non-invasive identification of plastic materials in museum collections with portable FTIR reflectance spectroscopy: Reference database and practical applications, Microchem. J. 124 (2016) 868–877. 10.1016/j.microc.2015.07.016.
7. M. Gómez, D. Reggio, M. Lazzari, Detection of Degradation Markers from Polymer Surfaces by a Novel SERS-Based Strategy, Talanta 191 (2019) 156–61. DOI: 10.1016/j.talanta.2018.08.046.
8. H. Zollinger, Color Chemistry: Syntheses, Properties, and Applications of Organic Dyes and Pigments, Wiley, 2003. https://doi.org/10.1002/anie.200385122.
9. S. Williams, Composition Implications of Plastic Objects: A Survey of Additives and Their Effects on the Longevity of Plastics. Proceedings of Conference Saving the Twentieth century: The Conservation of Modern Materials, Ottawa, Canada, 15 - 20 September 1991, D. Grattan (Eds.), Canadian Conservation Institute, 1993.
10. J. Lemaire, La prévision du comportement en long terme de matériaux polymères synthétiques dopais des experiences de vieillissement artificiel. Proc. Conference Saving the Twentieth century: The Conservation of Modern Materials, Ottawa, Canada, 15 - 20 September 1991, D. Grattan (Eds.), Canadian Conservation Institute, 1993.
11. P. P. Klemchuk, Influence of pigments on the light stability of polymers: A critical review, Polym. Photochem. 3 (1983), 1-27. https://doi.org/10.1016/0144-2880(83)90042-8.

12. S. Olivera, H. B. Muralidhara, K. Venkatesh, K. Gopalakrishna, C. S. Vivek, Plating on acrylonitrile-butadiene-styrene (ABS) plastic: a review, J. Mater. Sci. 51 (2016) 3657-3676. DOI: 10.1007/s10853-015-9668-7.
13. M. Baker, Mary T., and E. M. Manus, Spacesuits: NASA's Dream - Conservator's Nightmare, ln Proceedings of Conference Saving the Twentieth century: The Conservation of Modern Materials, Ottawa, Canada, 15 - 20 September 1991, D. Grattan (Eds.), Canadian Conservation Institute, 1993
14. D. Saviello, E. Pouvet, L. Toniolo, M. Cotte, A. Nevin, Synchrotron-based FTIR microspectroscopy for the mapping of photo-oxidation and additives in acrylonitrile-butadiene-styrene model samples and historical objects, Anal. Chim. Acta 843 (2014) 59-72. https://doi.org/10.1016/j.aca.2014.07.021.
15. C. Coon, B. Pretzel, T. Lomax, M. Strlič, Preserving Rapid Prototypes: A Review, Herit. Scie. 4, 1 (2016) 40. https://doi.org/10.1186/s40494-016-0097-y.
16. Claudia Hart, https://claudiahart.com/Mortifications-2007-2011, 2020 (accessed 19 May 2020)
17. S. W. Finch, Building-block US1191884A, 18-Jul-1916, https://patents.google.com, 2020 (accessed: 19 May 2020).
18. Patents - Hilary Page Toys, https://www.hilarypagetoys.com/Home/Patents, 2020 (accessed: 19 May 2020).
19. Home - LEGO.com US, https://www.lego.com/en-us/lego-history, 2020 (accessed: 19 May 2020).
20. G. K Christiansen., US751387A 19, https://patents.google.com/patent/US3005282A/en, 2020 (accessed: 19 May 2020).
21. D. Robertson and B. Breen, Brick by Brick: How LEGO Rewrote the Rules of Innovation and Conquered the Global Toy Industry. Crown, 2013.
22. S. Herman, A Million Little Objects: The Unofficial Illustrated History of the LEGO Phenomenon. Skyhorse Publishing, 2012
23. M. Lauwaert, Playing outside the box – on LEGO toys and the changing world of construction play. Hist. Technol. 24 (2008) 221-237. https://doi.org/10.1080/07341510801900300.
24. J. Kennedy, How are Lego® objects made? The Chemistry of LEGO®, https://jameskennedymonash.wordpress.com/2014/07/15/how-are-lego-objects-made-the-chemistry-of-lego/, 2014 (accessed: 19 May 2020).
25. Masader – Oman Virtual Science Library, Germany Petrochemicals Industry SnapShots https://www.masader.om/eds/detail?db=bsu&an=141268608, 2020 (accessed June 3, 2020)
26. Macrolex Red, https://techcenter.lanxess.com/fcc/emea/en/products/datasheet/MACROLEX_Red_EG_en.pdf?docId=21317916&gid=21316284&pid=21083592, 2020 (accessed June 3, 2020)
27. J. La Nasa, G. Biale, B. Ferriani, M. P. Colombini, F. Modugno, A Pyrolysis Approach for Characterizing and Assessing Degradation of Polyurethane Foam in Cultural Heritage Objects, J. Anal. Appl. Pyrolysis 134: (2018) 562–572. https://doi.org/10.1016/j.jaap.2018.08.004.
28. D. Scalarone, O., Chiantore, The use of Py-GC-MS for identification of the polymeric constituents in art works, museum and collectible design objects. In Plastic in Art: history, technology and preservation, Van Oosten, T. Shashoua, Y., Waenting, F., (Eds.) Verlag und Vertrieb: Munich, Germany, (2002) pp. 50–51.

29. A. Lattuati-Derieux, S. Thao-Heu, B. Lavédrine, Assessment of the Degradation of Polyurethane Foams after Artificial and Natural Ageing by Using Pyrolysis-Gas Chromatography/Mass Spectrometry and Headspace-Solid Phase Microextraction-Gas Chromatography/Mass Spectrometry, J. Chromatogr. A 1218 (28): (2011) 4498–4508. https://doi.org/10.1016/j.chroma.2011.05.013.
30. C. Kehlet, A. Catalano, J. Dittmer, Degradation of natural rubber in works of art studied by unilateral NMR and high field NMR spectroscopy, Polym. Degrad. Stabil. 107 (2014) 270-276. https://doi.org/10.1016/j.polymdegradstab.2013.12.039.
31. M. Lazzari, A. Ledo-Suárez, T. López, D. Scalarone, M. A. Quintela, Plastic matters: an analytical procedure to evaluate the degradability of contemporary works of art, Anal. Bioanal. Chem. 399 (2011) 2939-2948. DOI: 10.1007/s00216-011-4664-5.
32. G. Mitchell, F. France, A. Nordon, P. L. Tang, L. Gibson, Assessment of Historical Polymers Using Attenuated Total Reflectance-Fourier Transform Infra-Red Spectroscopy with Principal Component Analysis, Herit. Sci. 1 (1): (2013) 28. https://doi.org/10.1186/2050-7445-1-28.
33. V. Šuštar, J. Kolar, L. Lusa, T. Learner, M. Schilling, R. Rivenc, H. Khanjian, D. Koleša, Identification of Historical Polymers Using Near-Infrared Spectroscopy, Polym. Degrad. Stab. 107: (2014) 341–47. https://doi.org/10.1016/j.polymdegradstab.2013.12.035.
34. A. Pereira, Candeias, A. Cardoso, D. Rodriguez, P. Vandenabeele, A. T. Caldeira, Non-invasive methodology for the identification of plastic objects in museum environment — a novel approach, Microchem. J. 124 (2016), 846-855. DOI: 10.1016/j.microc.2015.07.027.
35. A. Klisińska-Kopacz, A. Mendys, J. M. Del Hoyo-Meléndez,B. Łydżba-Kopczyńska, P. Frączek, A. Kłosowska-Klechowska, M. Obarzanowski, Portable Raman and NIR Systems for Identification of Plastics in Museum Collections. Proc. of RAA, 9th International Congress on the Application of Raman Spectroscopy In Art and Archaeology, Evora, Portugal, October, 24-27, (2017)
36. A. Klisińska-Kopacz, B. Łydżba-Kopczyńska, M. Czarnecka, T. Koźlecki, J. del H. Mélendez, A. Mendys, A. Kłosowska-Klechowska, M. Obarzanowski, P. Frączek, Raman spectroscopy as a powerful technique for the identification of polymers used in cast sculptures from museum collections, J. Raman Spectrosc. 50 (2019) 213–221. https://doi.org/10.1002/jrs.5407.
37. G. Howell, M. Edwards, J. M. Chalmers, Raman Spectroscopy in Archaeology and Art History, Royal Society of Chemistry, 2005. ISBN 978-1-78801-138-9
38. A. M. Committee and A. No 67, Raman spectroscopy in cultural heritage: Background paper, Anal. Methods, 7, 12, 2015, pp. 4844–4847. https://doi.org/10.1039/C5AY90036.
39. A. Cesaratto, M. Leona, F. Pozzi, Recent Advances on the Analysis of Polychrome Works of Art: SERS of Synthetic Colorants and Their Mixtures with Natural Dyes, Front. Chem. 7 (2019) 105. https://doi.org/10.3389/fchem.2019.00105.
40. D. Bersani, C. Conti, P. L. Matousek, F. Pozzi, P. Vandenabeele, Methodological Evolutions of Raman Spectroscopy in Art and Archaeology, Anal. Methods 8 (48): 2016, 8395–8409. https://doi.org/10.1039/C6AY02327D.
41. S.A. Centeno, Identification of artistic materials in paintings and drawings by Raman spectroscopy: some challenges and future outlook, J. Raman Spectrosc. 47 (2016) 9–15. https://doi.org/10.1002/jrs.4767.
42. F. Schulte, K. W. Brzezinka, K. Lutzenberger, H. Stege, U. Panne, Raman Spectroscopy of Synthetic Organic Pigments Used in 20th Century Works of Art, J. Raman Spectrosc. 39, 10 (2008): 1455–63. https://doi.org/10.1002/jrs.2021.

43. F. Casadio, C. Daher, L. Bellot-Gurlet, Raman Spectroscopy of cultural heritage Materials: Overview of Applications and New Frontiers in Instrumentation, Sampling Modalities, and Data Processing, Top Curr. Chem. (Z). 374 (2016) 62. https://doi.org/10.1007/s41061-016-0061-z.
44. A. Quye, M. Strlič Ethical Sampling Guidance; Institute of Conservation: London, UK, 2019 https://icon.org.uk/system/files/documents/icon_hsg_ethical_sampling_guidance_-_jan_2019.pdf , 2020 (accessed June 3, 2020)
45. P. Vandenabeele, K. Castro, M. Hargreaves, L. Moens, J.M. Madariaga, H.G.M. Edwards, Comparative study of mobile Raman instrumentation for art analysis, Analytic. Chim. Acta. 588 (2007) 108–116. https://doi.org/10.1016/j.aca.2007.01.082.
46. Sawaya - Global exhibition using LEGO objects as an art medium by Nathan Sawaya http://www.nathansawaya.com/, 2020 (accessed June 3, 2020)
47. Ai Wewei, https://www.youtube.com/watch?v=zzwV49vRjFw, 2020 (accessed June 3, 2020)
48. Eliasson – Collectivity Project - High Line New York City artists using LEGO by Olefur Eliasson objects in exhibitions https://olafureliasson.net/archive/artwork/WEK100711/the-collectivity-project, 2020 (accessed June 3, 2020)
49. M. Lotts. On the Road, Playing with LEGO, and Learning about the Library: The Rutgers Art Library Lego Playing Station, Part Two. Jour. Libr Admin 56(5), (2016) 499- 525. http://dx.doi.org/10.1080/01930826.2016.1179517.
50. M. Gómez, S., Kadkhodazadeh, M. Lazzari, Surface-enhanced Raman Scattering (SERS) in the Visible Range on Scalable Aluminum- coated Platforms, Chem. Comm. 54 (2018) 10638–10641. https://doi.org/10.1039/C8CC04280B.
51. M. Gómez, D. Reggio, M. Lazzari. Linseed Oil as a Model System for Surface Enhanced Raman Spectroscopy Detection of Degradation Products in Artworks, J. Raman Spectrosc. 50 (2019) 242–49. https://doi.org/10.1002/jrs.5472.
52. Infrared and Raman Users Group (IRUG) Spectral Database, Available at: http://www.irug.org/search-spectral-database?reset=Reset, 2007 (accessed June 3, 2020)
53. W. Fremout, S. Saverwyns, Identification of Synthetic Organic Pigments: The Role of a Comprehensive Digital Raman Spectral Library, J. Raman Spectrosc. 43 (2012) 1536–1544. https://doi.org/10.1002/jrs.4054.
54. H. Zweifel, S.E. Amos, Plastics Additives Handbook, Hanser Gardner Publications, 2001.
55. J. Murphy, Ed., Front Matter, In Additives for Plastics Handbook, Amsterdam: Elsevier Science, 2001.
56. G. de la Torre, G. Bottari, U. Hahn, T. Torres. Functional Phthalocyanines: Synthesis, Nanostructuration, and Electro-Optical Applications, Funct. Phthalocyanine Mol. Mater., J. Jiang (Eds.), 135: 2010, pp.1-44. https://doi.org/10.1007/978-3-642-04752-7_1.
57. C. Defeyt, P. Vandenabeele, B. Gilbert, J. Van Pevenage, R, Cloots and D. Strivay, Contribution to the Identification of α-, β- and ε-Copper Phthalocyanine Blue Pigments in Modern Artists' Paints by X-Ray Powder Diffraction, Attenuated Total Reflectance Micro-Fourier Transform Infrared Spectroscopy and Micro-Raman Spectroscopy, J. Raman Spectrosc. 43 (2012), 1772-1780. https://doi.org/10.1002/jrs.4125.
58. C. Zimmerer, I. Matulaitiene, G. Niaura, U. Reuter, A. Janke, R. Boldt, V. Sablinskas, G. Steiner. Nondestructive Characterization of the Polycarbonate - Octadecylamine Interface by Surface Enhanced Raman Spectroscopy, Polymer Testing 73 (2019) 152–158. https://doi.org/10.1016/j.polymertesting.2018.11.023.

59. J. Gardette, B. Mailhot, J. Lemaire. Photooxidation Mechanisms of Styrenic Polymers. Polym. Degrad. Stabil, 48, (1995): 457–70. https://doi.org/10.1016/0141-3910(95)00113-Z.
60. Fourier transform Raman spectroscopy, Physical Sciences Data, Elsevier, 1998: pp. 18-20. ISBN: 978-0-444-82620-6.
61. D. Comelli, F. Toja, C. D'Andrea, L. Toniolo, G. Valentini, M. Lazzari, A. Nevin. Advanced Non-Invasive Fluorescence Spectroscopy and Imaging for Mapping Photo-Oxidative Degradation in Acrylonitrile–Butadiene–Styrene: A Study of Model Samples and of an Object from the 1960s, Polym. Degrad. Stab. 107 (sup. C) 2014: 356–65. https://doi.org/10.1016/j.polymdegradstab.2013.12.030.